

Toward a Unified Parameterization of the Boundary Layer and Moist Convection. Part I: A New Type of Mass-Flux Model

CARA-LYN LAPPEN AND DAVID A. RANDALL

Department of Atmospheric Sciences, Colorado State University, Fort Collins, Colorado

(Manuscript received 18 July 2000, in final form 31 January 2001)

ABSTRACT

Higher-order closure (HOC) models have been proposed for parameterization of the turbulent planetary boundary layer (PBL). HOC models must include closures for higher-order moments (e.g., fourth moments in third-order closure models), for pressure terms, and for dissipation terms. Mass-flux closure (MFC) models have been proposed for parameterization of cumulus convection and, more recently, the convective PBL. MFC models include closures for lateral mass exchanges and for pressure terms (which are usually ignored). The authors developed a new kind of model that combines HOC and MFC, which they hope will be useful for the parameterization of *both* the PBL and cumulus convection, in a unified framework. Such a model is particularly well suited to regimes in which the PBL turbulence and the cumulus convection are not well separated, for example, the broken stratocumulus and shallow cumulus regimes.

The model makes use of an assumed joint probability distribution for the variables of interest, and the equations typically used in HOC models can be derived by integrating over the distribution. Accordingly, the model is called Assumed-Distribution Higher-Order Closure (ADHOC). The prognostic variables of ADHOC are the mean state, the second and third moments of the vertical velocity, and the vertical fluxes of other quantities of interest. All of the parameters of the distribution can be determined from the predicted moments; thereafter the joint distribution is effectively known, and so any and all moments can be constructed as needed. In this way, the usual closure problem of “higher moments” is avoided. The pressure-term parameterizations previously developed for HOC models are used to predict the convective fluxes and the moments of the vertical velocity.

In companion papers, parameterizations of lateral mass exchanges and subplume-scale fluxes are presented, and then ADHOC is applied to several observationally based tropical, subtropical, and dry convective boundary layers.

1. Introduction

Many general circulation models (GCMs) currently use separate schemes for planetary boundary layer (PBL) processes, shallow and deep cumulus convection, and stratiform clouds. In reality these processes are not always distinct. For example, in the stratocumulus-to-cumulus transition region, stratocumulus clouds have been observed to break up into a combination of shallow cumulus and broken stratocumulus. Shallow cumulus clouds may be considered to reside completely within the PBL, or they may be regarded as starting in the PBL but terminating above it. Deeper cumulus clouds often originate within the PBL but can also originate aloft.

In this paper we present the basic structure of a parameterization, which, we believe, has the potential to represent boundary layer turbulence, shallow cumulus convection, and possibly even deep cumulus convection, all within a unified framework. Our approach is to

unify higher-order closure (HOC, a PBL parameterization) and mass-flux closure (MFC, a parameterization originally developed to represent the effects of cumulus convection). In this way, we can draw from two substantial preexisting knowledge bases to create one model—an exercise in “cross-fertilization.”

Parameterization of higher moments that appear in lower-order equations (the “closure problem”; Keller and Friedman 1924; Stull 1988) has been the focus of much atmospheric turbulence research. In the HOC equations, there are three classes of terms for which “closure” assumptions are needed. These are the higher moments that appear as transport terms in the lower-moment equations, the pressure–velocity correlations, and the dissipation terms.

The simplest closure assumption for fluxlike moments is that they always point down the gradient of the quantity being transported; this is “*K* theory.” Under convective conditions, however, PBL eddies can be very deep, and the associated fluxes are often countergradient (Deardorff 1966; Wyngaard and Coté 1974; Zeman and Lumley 1976). Thus, attempts have been made to modify *K* theory so as to allow countergradient fluxes under

Corresponding author address: Dr. Cara-Lyn Lappen, Department of Atmospheric Science, Colorado State University, Fort Collins, CO 80523.
E-mail: lappen@atmos.colostate.edu

some conditions. Examples include 1) the addition of a countergradient term to represent the nonlocal aspects of the flow (Deardorff 1966; Mailhot and Benoit 1982; Therry and Lecarré 1983; Troen and Mahrt 1986; Holtslag and Moeng 1991); 2) transilience turbulence theory, which permits simultaneous mixing between any and all pairs of levels (Stull 1988); and 3) spectral diffusivity theory, in which the mixing coefficient is assumed to scale with the size of the eddy, and the diffusion equations are spectrally decomposed (Berkowicz and Prahm 1979). In large-scale models for which lower-order schemes are adopted, often one of these modified K theories is chosen to represent fluxes. Examples include the K -profile parameterization of Troen and Mahrt (1986), which is used in the National Center for Atmospheric Research (NCAR) Community Climate Model version 3 (Holtslag and Boville 1993), and the K -Richardson-number-dependent model of Louis (1979), which is used in the European Centre for Medium-Range Weather Forecasts model.

To the best of our knowledge, no “nonlocal” parameterization exists for the corresponding “fluxlike” (third moment) terms in the second-moment equations, other than third-order closure itself (André et al. 1978). Most current models parameterize the third moments with a simple downgradient diffusion assumption with various formulas for the eddy diffusivity (e.g., Moeng and Wyngaard 1989). Surely, a more realistic way to represent the effects of the third moments could greatly improve the realism of PBL models.

Parameterizations for the pressure terms were pioneered by Rotta (1951a,b), who broke them down into “pressure-transport” and “return-to-isotropy” terms. He neglected the former and assumed that the role of the latter is to drive the turbulence toward an isotropic state. Later, it was realized that neglect of the pressure-transport term is a serious error (Naot et al. 1973; Wyngaard and Coté 1974; Lumley and Khajeh Nouri 1974; Launder 1975; Zeman and Lumley 1976). By 1990, it had become clear that the pressure-transport terms are important, especially in the surface and inversion regions of the boundary layer where the vertically moving air is forced to slow down (Canuto 1992). For example, the convergence of air as a downdraft approaches the surface creates high pressure, which acts to slow the air down and “splash” it out to the side. Conversely, updraft air near the surface creates a low pressure wake behind it. In current mass-flux models, the pressure terms are most often entirely neglected (although there are some exceptions, e.g., Wu and Yanai 1994).

The final closure needed by HOC models is for the rates of dissipation. Two paths have been taken in attempts to accurately represent the effects of turbulent dissipation. The first is to predict directly either the dissipation or a turbulent length scale directly (Langland and Liou 1996; Beljaars et al. 1987; Detering and Etling 1985), and the second is to diagnostically determine one of these quantities (e.g., Blackadar 1962; Bougeault and

André 1986; Canuto et al. 1994). A natural way to parameterize a dissipation rate is to make it proportional to the negative of what it supposed to dissipate; that is,

$$\frac{\partial \overline{x'y'}}{\partial t} \sim -\frac{\overline{x'y'}}{\tau}, \quad (1)$$

where τ is a dissipation timescale, and x and y are dummy variables. Equation (1) is nothing more than a definition of τ . The problem is then to parameterize τ .

HOC models have been more successful at simulating some regimes than others. This is because standard closures make use of the assumption that turbulence is nearly isotropic and nearly Gaussian (Lumley 1978), whereas some regimes (e.g., trade wind cumulus) are highly nonisotropic and non-Gaussian. In order to simulate the trade wind (TW) cumulus regime accurately, HOC models must be “tuned” (Randall and Wielicki 1997). For example, Bougeault (1981a) developed a special turbulence condensation scheme with the help of the large-eddy simulation (LES) results of Somméria (1976) for a 1D HOC simulation of the trade wind PBL. Bechtold et al. (1995) developed a scheme in which they linearly interpolated between the Gaussian turbulence profiles and a distribution with known constant positive vertical velocity skewness. He tuned the skewness to a trade wind-specific value, which gave satisfactory results.

In the late 1960s and early 1970s, boundary layer parameterizations (e.g., K theory, mixed-layer models, HOC) and mass-flux-based cumulus parameterizations (e.g., Arakawa 1969; Betts 1973; Arakawa and Schubert 1974) were being developed simultaneously but independently. Unlike HOC models, mass-flux models were specifically designed for cumulus regimes. MFC was pioneered by Arakawa (1969), who applied it to deep and shallow cumulus convection. Further applications of mass-flux ideas to cumulus convection were reported by Ooyama (1971), Arakawa and Schubert (1974), and Betts (1973).

MFC explicitly recognizes that, in order to satisfy mass continuity, compensating downdrafts must fill the space between the buoyant updrafts in a convective regime. Within the “classical” mass-flux framework, all dynamic and thermodynamic quantities are represented with tophat¹ profiles. Using tophat distributions, Arakawa partitioned the cumulus regime into two components: updrafts and the environment surrounding the updrafts. He then parameterized the fluxes as the product of a convective mass flux (M_c) and the difference in a quantity’s value between the updraft and the environment using

¹ A tophat profile is a probability distribution function that consists only of two delta functions. Thus, a quantity represented by a tophat profile has 100% probability of having one of just two possible values. In the simplest type of mass-flux model, the two allowed states are those of the updraft and downdraft.

$$\overline{mw'h'} = M_c(h_{\text{up}} - h_c). \quad (2)$$

Here m is the density of the air, $M_c = m\sigma w_{\text{up}}$, σ is the average fractional area of updrafts, and w_{up} is the average vertical velocity in updrafts. An assumption used in (2) (written here for a single cloud type) is that “large eddies” (eddies whose scales are comparable to or larger than the depth of the PBL) account for most of the turbulent transport in the cumulus regime. Since (2) explicitly distinguishes between “updrafts” and the “environment,” it entails the assumption that the environment is well defined. This is the case when the updraft area fraction is much less than unity. Later, many researchers applied this approach to the PBL and developed parameterizations that could be applied to both clear and cloudy convective boundary layers (Betts 1973, 1976; Albrecht 1979; Hanson 1981; Randall 1987; Wang and Albrecht 1986, 1990). Because the distinction between updraft and environment is not as clear for many boundary layer regimes, in which the updraft area fraction can be close to 1/2, these researchers reinterpreted Arakawa’s “updraft–environment” framework as an “updraft–downdraft” pair. They modified Arakawa’s parameterization [Eq. (2)] by replacing h_e with h_{dn} , the value of h in a convective downdraft. Thus, the flux of h is written as

$$\overline{mw'h'} = M_c(h_{\text{up}} - h_{\text{dn}}). \quad (3)$$

Subsequent studies have shown that (3) actually represents only 60% of the total flux in convective (Businger and Oncley 1990; Young 1988a; Schumann and Moeng 1991a; Wyngaard and Moeng 1992) and stratocumulus-topped boundary layers (Schumann and Moeng 1991a; Wang and Stevens 2000; de Laet and Duynkerke 1998), while it represents 80–90% of the total flux for conserved variables in cumulus layers (except near cloud base; Siebesma and Cuijpers 1995; Wang and Stevens, 2000). This percentage is considerably less for nonconserved variables in cumulus layers. All values can vary depending on the conditional sampling technique employed (Wang and Stevens 2000).

Observational studies (Nicholls and Lemone 1980; Greenhut and Khalsa 1982, 1987; Lenschow and Stephens 1980; Crum et al. 1987; Young 1988a,b) have advanced our understanding of the dynamics of thermals in the convective boundary layer (CBL); this has helped modelers working to incorporate (3) (with applications to both cloudy and clear regimes) into numerical models (e.g., Wang and Albrecht 1986; Chatfield and Brost 1987; Penc and Albrecht 1987). Mixed-layer models² have been combined with mass-flux models to simulate dry, convective (Wang and Albrecht 1990), and cloudy (Betts 1976; Albrecht 1979) PBLs. In addition, the ap-

plicability of MFC to nonconvective regimes is suggested by the observational study of Businger and Oncley (1990).

Wang and Albrecht (1990) simulated dry convection using prognostic equations only for the mean quantities in the updraft and downdraft. They found that their simple model was able to simulate the observed CBL more realistically than mixed-layer models. The major improvement over a mixed-layer model was the fact that it allowed for an explicit representation of processes that control gradients of conserved variables (e.g., internal mixing and lateral mixing between updraft and downdraft elements). Wang and Albrecht speculated that a unified cloud and PBL model could be developed with such an approach.

Mass-flux models have also met with some success in modeling the stratocumulus-topped and the TW cumulus PBLs. Penc and Albrecht (1987) used data from the NCAR Electra, which flew off the coast of California in June 1976, to show that (3) can be used to describe the stratocumulus-topped PBL (ScTBL). This was further confirmed recently by de Laet and Duynkerke (1998) using data from the Atlantic Stratocumulus Experiment. Most modeling studies of the ScTBL have employed mixed-layer models, along with the mass-flux parameterization (e.g., Wang and Albrecht 1986). Mass-flux schemes were also used in conjunction with mixed-layer models to simulate the TW cumulus layer by Betts (1973, 1976), Albrecht (1979), and Hanson (1981). The major shortcomings of these models are their mixed-layer assumption, which does not permit accurate representation of the internal structure of the PBL, and their inability to represent fractional cloudiness.

The mass-flux approach requires a method to determine the updraft area fraction σ and the mass flux M_c . To our knowledge, Randall et al. (1992, hereafter RSM) were the first to propose a physically based method to diagnose these quantities. They took steps toward combining MFC and HOC. In the present paper, we considerably extend the approach of RSM. For reasons that will become clear, we call the approach Assumed-Distribution Higher-Order Closure (ADHOC). In the spirit of earlier mass-flux models, RSM adopted a “tophat” probability density function (PDF; see footnote 1) to describe the mean-state and turbulent fluxes in the atmosphere. They derived expressions analogous to Eq. (3) for *all* higher-order terms (e.g., variances, other covariances, and third-order and higher moments). They showed that all higher moments can be represented in terms of various combinations of a convective mass flux and the difference in properties between updrafts and downdrafts.

As an example, suppose that h is an intensive property of a system (potential temperature, mixing ratio, etc.). With MFC, one can represent the mean value of h as an area-weighted average of its two components:

$$\bar{h} = \sigma h_{\text{up}} + (1 - \sigma) h_{\text{dn}}, \quad (4)$$

² Mixed-layer models are simplified first-order closure schemes (Ball 1960; Lilly 1968; Randall 1976; Benoit 1976). In mixed-layer models, the boundary layer is treated as a single layer and the turbulent flux profiles are computed from only the surface fluxes and the entrainment rate.

where σ is the fractional area covered by the updrafts, and h_{up} and h_{dn} are the values of h in the updraft and downdraft, respectively. RSM also introduced a convective mass flux,

$$M_c = m\sigma(1 - \sigma)(w_{\text{up}} - w_{\text{dn}}), \quad (5)$$

where $1 - \sigma$ is the fractional downdraft area, and $(w_{\text{up}} - w_{\text{dn}})$ is the difference in the vertical velocity between the updraft and downdraft.

RSM used (4)–(5) to derive expressions for higher moments. For example, we can derive an expression for the vertical flux of h by replacing h with $w'h'$ in (4); this gives

$$m\overline{w'h'} = m[\sigma w'_{\text{up}} h'_{\text{up}} + (1 - \sigma)w'_{\text{dn}} h'_{\text{dn}}]. \quad (6)$$

Substituting the expressions $h'_{\text{up}} = h_{\text{up}} - \bar{h}$ and $h'_{\text{dn}} = h_{\text{dn}} - \bar{h}$ (along with the analogous ones for vertical velocity perturbations) and simplifying, we can obtain the mass-flux formula (3).

One can follow similar procedures to obtain expressions for variances; that is,

$$m\overline{h'h'} = m\sigma(1 - \sigma)(h_{\text{up}} - h_{\text{dn}})^2 \quad (7)$$

and other higher-order moments:

$$m\overline{w'h'h'} = m\sigma(1 - \sigma)(1 - 2\sigma) \times (w_{\text{up}} - w_{\text{dn}})(h_{\text{up}} - h_{\text{dn}})^2, \quad (8)$$

$$m\overline{w'h'h'h'} = m\sigma(1 - \sigma)(1 - 3\sigma + 3\sigma^2) \times (w_{\text{up}} - w_{\text{dn}})(h_{\text{up}} - h_{\text{dn}})^3. \quad (9)$$

In short, we can use this approach to diagnostically determine any higher moments that appear in the turbulence closure equations, provided that the variables of the mass-flux model are known.

Two of the variables that we need to determine are σ and M_c . The approach of RSM provides us with a physically based method to diagnose these quantities. In (4), (7), and (8), we replace h by w everywhere. In doing so, we are left on the rhs with three equations and three unknowns: w_{up} , w_{dn} , and σ . Solving this system of equations, we find that

$$\sigma = \frac{1}{2} - \frac{S_w}{2(4 + S_w^2)^{1/2}}, \quad (10)$$

$$M_c = \rho\sigma(1 - \sigma)(w_{\text{up}} - w_{\text{dn}}) = \frac{m(w'^2)^{1/2}}{(4 + S_w^2)^{1/2}}, \quad (11)$$

where

$$S_w = \frac{\overline{w'^3}}{(\overline{w'^2})^{3/2}} \quad (12)$$

is the skewness of the vertical velocity. This demonstrates that given $\overline{w'^2}$ and $\overline{w'^3}$, we can diagnose both σ and M_c . To completely “close” this system, however, we must also know the difference in properties between the updrafts and downdrafts of all variables of interest

[Eqs. (6)–(9)]. We can determine these if we know the flux and the mean value of the desired variable [Eqs. (4) and (6)]. The success of this method thus *requires* the knowledge of certain higher-moment statistics, namely, $\overline{w'^2}$, $\overline{w'^3}$, and the vertical flux of any model variable. RSM proposed using HOC equations to determine these quantities. A schematic illustrating this logic is shown in Fig. 1.

As an example, consider a model containing two thermodynamic variables, representing energy and moisture. In order to apply the approach described here in such a model, we require only four higher-order closure equations (for $\overline{w'^2}$, $\overline{w'^3}$, and the two thermodynamic fluxes), plus equations for the mean state. For comparison, in a “conventional” third-order closure model with two thermodynamic variables, 10 second- and third-order moments must be predicted (e.g., Stull 1988). We should note that since subplume-scale (SPS) contributions are removed by tophat filtering, we include an additional equation for the SPS turbulent kinetic energy (see Part II, Lappen and Randall 2001a, hereafter LR2).

Moreover, in ADHOC, all of the various moments are *guaranteed* to be “realizable” because they are all diagnosed from the same PDF. In conventional HOC models, there is nothing to guarantee realizability (Andre et al. 1976).

We can summarize the advantages of the ADHOC approach as follows:

- 1) all of the higher-order statistics are guaranteed to be consistent with one another;
- 2) the model provides a physical basis for determining σ and M_c ;
- 3) many fewer prognostic equations are required compared with conventional HOC;
- 4) the model has an inherent ability to represent non-local transport³ and partial cloudiness.

The main weakness of the approach is the crudeness of the tophat assumption for dynamic and thermodynamic quantities.

In the present study, we use a plume model to derive prognostic equations for higher-moment statistics, based on Eqs. (6)–(9). We demonstrate that the resulting model, ADHOC, is exactly consistent with the standard HOC equations, in the sense that there is an exact term-by-term correspondence. For the pressure terms, we use

³ A mass-flux representation of the fluxes has many advantages over diffusion, especially in the convective PBL. With diffusion, transport occurs level by level and information flows simultaneously both upward and downward in the boundary layer. With mass-flux closure, information either flows up (if σ is small) or down (if σ is large). It is similar to advection in that information flows in whatever direction the “velocity” is moving. We can say that local transport is diffusive, while nonlocal transport (like that described by mass-flux closure) is advective. In a cumulus layer (where σ is very small), the transport is clearly not diffusive. Thus, mass-flux closure is distinctly more realistic than diffusion closure for the representation of higher-moment transport terms.

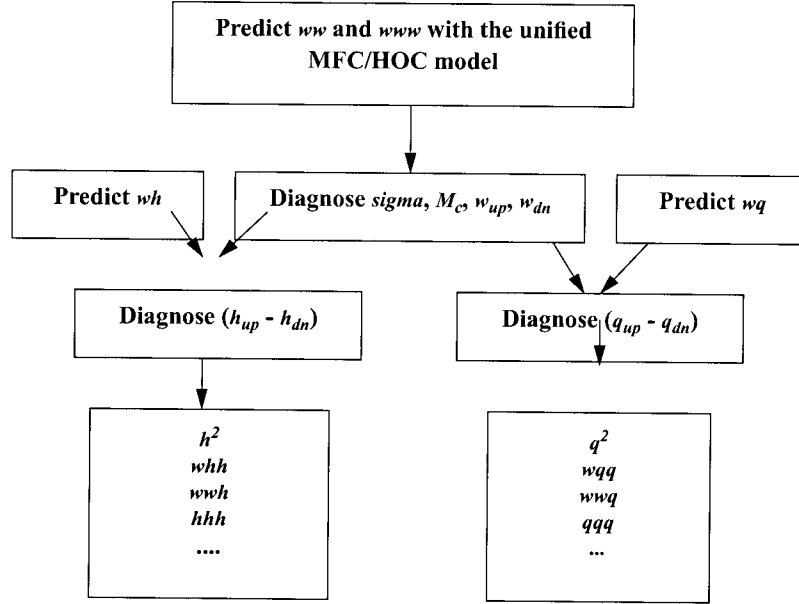


FIG. 1. ADHOC model logic, based on RSM. We use ww and www to predict σ , M_c , w_{up} , and w_{dn} using (10)–(11). We then predict the flux of a variable and use (3) to diagnose the difference in properties of the variable between the updraft and downdraft. Finally, we use equations of the form (7)–(9) to diagnose any other higher moment.

parameterizations that have been developed for HOC; most MFC models have neglected these terms entirely. To determine the dissipation terms, we use ideas from both HOC and MFC.

The remainder of the paper is organized as follows. In section 2, we derive the governing equations. This includes a discussion of the ADHOC-consistent second- and third-moment equations, and their reduction to known HOC and MFC relationships for some limiting cases. In sections 3 and 4, we discuss the manner in which momentum and pressure correlations are handled in ADHOC. In section 6, we draw conclusions, and discuss the possible wider applicability of our approach. In LR2, we present a new parameterization of the lateral mass exchange terms, and discuss an SPS parameterization, which we incorporate into ADHOC in order to represent the small-eddy contribution to the flow. In Part III (Lappen and Randall 2001b, hereafter LR3), we show some results from simulations of a variety of clear and cloudy PBL regimes.

2. Governing equations

a. Framework

Following RSM, we distinguish between the rising and sinking regions of grid cells. Accordingly, we divide a grid cell into two subregions, denoted by subscripts “up” and “dn,” with areas A_{up} and A_{dn} , respectively. We assume that

$$A_{up} + A_{dn} = A. \quad (13)$$

Here A (no subscript) is the total area of the grid cell.

If we consider an arbitrary intensive variable h and let S_h denote the source or sink of h , we can write the following budget equations:

$$\begin{aligned} \frac{\partial}{\partial t}(mh_{up}A_{up}) &= EA_{dn} - DA_{up} - \frac{\partial}{\partial z}(mw_{up}h_{up}A_{up}) \\ &\quad + m(S_h)_{up}A_{up}, \end{aligned} \quad (14)$$

$$\begin{aligned} \frac{\partial}{\partial t}(mh_{dn}A_{dn}) &= DA_{up} - EA_{dn} - \frac{\partial}{\partial z}(mw_{dn}h_{dn}A_{dn}) \\ &\quad + m(S_h)_{dn}A_{dn}, \end{aligned} \quad (15)$$

where E (D) is the lateral mass exchange from the sinking (rising) air into the rising (sinking) air, and m is the density of the air. We ignore density differences between the updrafts and downdrafts, except for buoyancy effects, which are discussed later. Advection by the mean flow is neglected here for simplicity although it can be included as shown by Lappen (1999).

In view of the definitions of E and D ,

$$D \geq 0 \quad \text{and} \quad E \geq 0. \quad (16)$$

Note that D is *not* equal to minus E . The two mass exchange processes can occur independently and simultaneously. A full discussion of the parameterization of E and D is given in LR2.

When we add (14) and (15), the E and D terms cancel out and we obtain

$$\frac{\partial}{\partial t}m\bar{h} = -\frac{\partial}{\partial z}m\overline{wh} + m\overline{(S_h)}, \quad (17)$$

where

$$\overline{h}A = h_{\text{up}}A_{\text{up}} + h_{\text{dn}}A_{\text{dn}}, \quad (18)$$

$$\overline{mwh}A = mw_{\text{up}}h_{\text{up}}A_{\text{up}} + mw_{\text{dn}}h_{\text{dn}}A_{\text{dn}}, \quad \text{and} \quad (19)$$

$$\overline{(S_h)A} = (S_h)_{\text{up}}A_{\text{up}} + (S_h)_{\text{dn}}A_{\text{dn}}. \quad (20)$$

The continuity equations corresponding to (14)–(15) and (17) can be obtained by setting $h = 1$ and $S_h = 0$:

$$\frac{\partial}{\partial t}(mA_{\text{up}}) = EA - DA - \frac{\partial}{\partial z}(mw_{\text{up}}A_{\text{up}}), \quad (21)$$

$$\frac{\partial}{\partial t}(mA_{\text{dn}}) = DA - EA - \frac{\partial}{\partial z}(mw_{\text{dn}}A_{\text{dn}}), \quad (22)$$

$$\frac{\partial m}{\partial t} = -\frac{\partial}{\partial z}m\overline{w}, \quad (23)$$

where \overline{w} is the area-averaged vertical velocity. Equations (21)–(22) govern the time change of the mass or area within each subregion. Equation (23) is the continuity equation for a whole grid cell. The horizontal advection term is missing in (23) because we neglected advection by the mean flow in (14)–(15).

For convenience, we define

$$\sigma \equiv \frac{A_{\text{up}}}{A}. \quad (24)$$

Using (13) and (24), we find that

$$1 - \sigma = \frac{A_{\text{dn}}}{A}. \quad (25)$$

With this definition of σ , we can show that

$$w_{\text{up}} = \overline{w} + (1 - \sigma)(w_{\text{up}} - w_{\text{dn}}), \quad (26)$$

$$w_{\text{dn}} = \overline{w} - \sigma(w_{\text{up}} - w_{\text{dn}}), \quad \text{and} \quad (27)$$

$$\begin{aligned} \overline{mwh} &= mw_{\text{up}}h_{\text{up}}\sigma + mw_{\text{dn}}h_{\text{dn}}(1 - \sigma) \\ &= m\overline{w}\overline{h} + M_c(h_{\text{up}} - h_{\text{dn}}). \end{aligned} \quad (28)$$

In (28), $m\overline{w}$ is the “large-scale” mass flux, and M_c is the convective mass flux given by (5). Equation (28) shows that each of these mass fluxes contributes to the total vertical flux of any quantity.

By combining (21)–(23) and (28) with (14)–(15) and (17), we can derive “advective forms” of the budget equations for h :

$$\begin{aligned} mA_{\text{up}}\frac{\partial h_{\text{up}}}{\partial t} &= EA(h_{\text{dn}} - h_{\text{up}}) - mA_{\text{up}}w_{\text{up}}\frac{\partial h_{\text{up}}}{\partial z} \\ &\quad + m(S_h)_{\text{up}}A_{\text{up}}, \end{aligned} \quad (29)$$

$$\begin{aligned} mA_{\text{dn}}\frac{\partial h_{\text{dn}}}{\partial t} &= DA(h_{\text{up}} - h_{\text{dn}}) - mA_{\text{dn}}w_{\text{dn}}\frac{\partial h_{\text{dn}}}{\partial z} \\ &\quad + m(S_h)_{\text{dn}}A_{\text{dn}}, \end{aligned} \quad (30)$$

$$\begin{aligned} m\frac{\partial \overline{h}}{\partial t} &= -m\overline{w}\frac{\partial \overline{h}}{\partial z} - \frac{\partial}{\partial z}[M_c(h_{\text{up}} - h_{\text{dn}})] \\ &\quad + m\overline{(S_h)}. \end{aligned} \quad (31)$$

b. Second and third moments

In this section, we derive the second- and third-moment equations, starting from the equations for the updraft and downdraft properties. We will do this for $w'h'$, $w'w'$, and $w'w'w'$. We show that the resulting equations are term-by-term consistent with the corresponding HOC equations:

$$\begin{aligned} \frac{\partial}{\partial t}\overline{w'h'} &= -\frac{1}{m}\frac{\partial}{\partial z}\overline{mw'w'h'} - \overline{w'w'}\frac{\partial \overline{h}}{\partial z} \\ &\quad + \frac{g}{C_p T_0}\overline{h's'_v} - \frac{1}{m}h'\frac{\partial p'}{\partial z} - \varepsilon_{wh}, \end{aligned} \quad (32)$$

$$\begin{aligned} \frac{\partial}{\partial t}\overline{w'w'} &= -\frac{1}{m}\frac{\partial}{\partial z}\overline{mw'w'w'} + 2\frac{g}{C_p T_0}\overline{w's'_v} \\ &\quad - \varepsilon_{ww} - \frac{2}{m}w'\frac{\partial p'}{\partial z}, \end{aligned} \quad (33)$$

$$\begin{aligned} \frac{\partial}{\partial t}\overline{w'w'w'} &= -\frac{1}{m}\frac{\partial}{\partial z}\overline{mw'w'w'w'} + \frac{3}{m}w'^2\frac{\partial}{\partial z}(\overline{mw'w'^2}) \\ &\quad + 3\frac{g}{C_p T_0}\overline{w's'_v} - \varepsilon_{www} - \frac{3}{m}w'^2\frac{\partial p'}{\partial z}, \end{aligned} \quad (34)$$

where w is the vertical velocity, h is an any intensive variable, C_p is the heat capacity of air at constant pressure, g is the acceleration of gravity, T_0 is a reference temperature, $s_v = C_p T_v + gz - L_v r_L$ is the virtual liquid water static energy, T_v is the virtual temperature, z is height, L_v is the latent heat of condensation of water vapor, r_L is the liquid water mixing ratio, ε_x is the rate of dissipation of a dummy variable x , and p is pressure.

To derive the second- and third-moment equations, we begin by expanding the left-hand sides of (32)–(34) following the approach of RSM:

$$\begin{aligned} \frac{\partial}{\partial t}[\sigma(1 - \sigma)(w_{\text{up}} - w_{\text{dn}})^2] &= (w_{\text{up}} - w_{\text{dn}})^2(1 - 2\sigma)\frac{\partial \sigma}{\partial t} \\ &\quad + 2\sigma(1 - \sigma)(w_{\text{up}} - w_{\text{dn}})\frac{\partial}{\partial t}(w_{\text{up}} - w_{\text{dn}}), \end{aligned} \quad (35)$$

$$\begin{aligned} \frac{\partial}{\partial t}[\sigma(1 - \sigma)(w_{\text{up}} - w_{\text{dn}})(h_{\text{up}} - h_{\text{dn}})] &= (w_{\text{up}} - w_{\text{dn}})(h_{\text{up}} - h_{\text{dn}})(1 - 2\sigma)\frac{\partial \sigma}{\partial t} \\ &\quad + \sigma(1 - \sigma)\frac{\partial}{\partial t}[(w_{\text{up}} - w_{\text{dn}})(h_{\text{up}} - h_{\text{dn}})], \end{aligned} \quad (36)$$

$$\begin{aligned} \frac{\partial}{\partial t}[\sigma(1 - \sigma)(1 - 2\sigma)(w_{\text{up}} - w_{\text{dn}})^3] &= (w_{\text{up}} - w_{\text{dn}})^3[6\sigma^2 - 6\sigma + 1]\frac{\partial \sigma}{\partial t} \end{aligned}$$

$$\begin{aligned}
& + 3\sigma(1 - \sigma)(1 - 2\sigma)(w_{\text{up}} - w_{\text{dn}})^2 \\
& \times \frac{\partial}{\partial t}(w_{\text{up}} - w_{\text{dn}}). \tag{37}
\end{aligned}$$

From (29) and (30), we can derive an equation for the time change of the updraft–downdraft difference, $h_{\text{up}} - h_{\text{dn}}$:

$$\begin{aligned}
\frac{\partial}{\partial t}(h_{\text{up}} - h_{\text{dn}}) = & -\left(\frac{E}{\sigma} + \frac{D}{1 - \sigma}\right)\frac{(h_{\text{up}} - h_{\text{dn}})}{m} - w_{\text{up}}\frac{\partial h_{\text{up}}}{\partial z} \\
& + w_{\text{dn}}\frac{\partial h_{\text{dn}}}{\partial z}(S_h)_{\text{up}} - (S_h)_{\text{dn}}. \tag{38}
\end{aligned}$$

We can write an essentially identical equation for the vertical velocity difference,

$$\begin{aligned}
\frac{\partial}{\partial t}(w_{\text{up}} - w_{\text{dn}}) = & -\left(\frac{E}{\sigma} + \frac{D}{1 - \sigma}\right)\frac{(w_{\text{up}} - w_{\text{dn}})}{m} \\
& - \frac{1}{2}\frac{\partial}{\partial z}[(w_{\text{up}})^2 - (w_{\text{dn}})^2] \\
& + [(S_w)_{\text{up}} - (S_w)_{\text{dn}}], \tag{39}
\end{aligned}$$

where $(S_w)_{\text{up}}$ and $(S_w)_{\text{dn}}$ represent the sources and sinks of w in the updraft and downdraft, respectively. The difference between these two quantities is

$$\begin{aligned}
& (S_w)_{\text{up}} - (S_w)_{\text{dn}} \\
& = \frac{g}{T_0}(T_{\text{up}} - T_{\text{dn}}) - \frac{1}{m}\frac{\partial}{\partial z}(p_{\text{up}} - p_{\text{dn}}) \\
& - \left\{ \frac{1}{\sigma}\frac{\partial}{\partial z}(\overline{\sigma w' w'}_{\text{sps,up}}) \right. \\
& \quad \left. - \frac{1}{(1 - \sigma)}\frac{\partial}{\partial z}[(1 - \sigma)\overline{w' w'}_{\text{sps,dn}}] \right\}. \tag{40}
\end{aligned}$$

The terms on the right-hand side of (40) represent (from right to left) buoyancy, pressure, and SPS effects. The parameterization of the pressure terms is discussed in section 4. The SPS terms are addressed in LR2.

From (38) and (39) we can form a prognostic equation for $(w_{\text{up}} - w_{\text{dn}})(h_{\text{up}} - h_{\text{dn}})$:

$$\begin{aligned}
& \frac{\partial}{\partial t}[(w_{\text{up}} - w_{\text{dn}})(h_{\text{up}} - h_{\text{dn}})] \\
& = -2\left(\frac{E}{\sigma} + \frac{D}{1 - \sigma}\right)\frac{(w_{\text{up}} - w_{\text{dn}})(h_{\text{up}} - h_{\text{dn}})}{m} \\
& - \frac{(h_{\text{up}} - h_{\text{dn}})}{2}\frac{\partial}{\partial z}[(w_{\text{up}})^2 - (w_{\text{dn}})^2] \\
& + (w_{\text{up}} - w_{\text{dn}})\left[-w_{\text{up}}\frac{\partial h_{\text{up}}}{\partial z} + w_{\text{dn}}\frac{\partial h_{\text{dn}}}{\partial z}\right] \\
& + (h_{\text{up}} - h_{\text{dn}})[(S_w)_{\text{up}} - (S_w)_{\text{dn}}] \\
& + (w_{\text{up}} - w_{\text{dn}})[(S_h)_{\text{up}} - (S_h)_{\text{dn}}]. \tag{41}
\end{aligned}$$

This immediately carries over to

$$\begin{aligned}
& \frac{\partial(w_{\text{up}} - w_{\text{dn}})^2}{\partial t} \\
& = -2\left(\frac{E}{\sigma} + \frac{D}{1 - \sigma}\right)\frac{(w_{\text{up}} - w_{\text{dn}})^2}{m} \\
& - (w_{\text{up}} - w_{\text{dn}})\frac{\partial}{\partial z}[(w_{\text{up}})^2 - (w_{\text{dn}})^2] \\
& + 2(w_{\text{up}} - w_{\text{dn}})[(S_w)_{\text{up}} - (S_w)_{\text{dn}}]. \tag{42}
\end{aligned}$$

Finally, using the identity $\partial A^3/\partial t = 3A^2(\partial A/\partial t)$, we can write

$$\begin{aligned}
& \frac{\partial(w_{\text{up}} - w_{\text{dn}})^3}{\partial t} \\
& = -3\left(\frac{E}{\sigma} + \frac{D}{1 - \sigma}\right)\frac{(w_{\text{up}} - w_{\text{dn}})^3}{m} \\
& - \frac{3}{2}(w_{\text{up}} - w_{\text{dn}})^2\frac{\partial}{\partial z}[(w_{\text{up}})^2 - (w_{\text{dn}})^2] \\
& + 3(w_{\text{up}} - w_{\text{dn}})^2[(S_w)_{\text{up}} - (S_w)_{\text{dn}}]. \tag{43}
\end{aligned}$$

We now recast the continuity equations [Eqs. (21)–(22)] for the updrafts and downdrafts. Making use of the definition of σ [Eq. (24)], and in the spirit of the anelastic approximation, neglecting the tendency of m , we obtain

$$\frac{\partial \sigma}{\partial t} = \frac{E - D}{m} - \frac{1}{m}\frac{\partial}{\partial z}(mw_{\text{up}}\sigma), \tag{44}$$

$$\frac{\partial}{\partial t}(1 - \sigma) = \frac{D - E}{m} - \frac{1}{m}\frac{\partial}{\partial z}[mw_{\text{dn}}(1 - \sigma)]. \tag{45}$$

We would like to combine (44) and (45) into a symmetrical form. Multiply (45) by σ , and subtract the result from $(1 - \sigma)$ times (44), to obtain

$$\frac{\partial \sigma}{\partial t} = \left(\frac{E - D}{m}\right) - \frac{1}{m}\frac{\partial M_c}{\partial z} - \bar{w}\frac{\partial \sigma}{\partial z}. \tag{46}$$

Here we have used (5) and $\bar{w} = \sigma w_{\text{up}} + (1 - \sigma)w_{\text{dn}}$.⁴ In the second- and third-moment equations, we neglect the effects of the mean vertical velocity, so that we approximate (46) by

$$\frac{\partial \sigma}{\partial t} = \left(\frac{E - D}{m}\right) - \frac{1}{m}\frac{\partial M_c}{\partial z}. \tag{47}$$

Now we assemble the various pieces to form the second- and third-moment equations, beginning with the equation for the vertical velocity variance [Eq. (35)]. The details of this derivation are given by Lappen (1999). The result is

⁴ We ignore the antisymmetric part of Eqs. (44)–(45) (obtained by adding these equations) because it gives only the continuity equation for the mean flow.

$$\begin{aligned}
& \frac{\partial}{\partial t} [m\sigma(1 - \sigma)(w_{\text{up}} - w_{\text{dn}})^2] \\
&= -(w_{\text{up}} - w_{\text{dn}})^2(E + D) \\
&\quad - \frac{\partial}{\partial z} [M_c(1 - 2\sigma)(w_{\text{up}} - w_{\text{dn}})^2] \\
&\quad + 2M_c[(S_w)_{\text{up}} - (S_w)_{\text{dn}}]. \quad (48)
\end{aligned}$$

We can identify the terms on the right-hand side of (48) as dissipation, transport, and the effects of sources and sinks associated with buoyancy, pressure forces, and small-scale mixing [see Eq. (40)]. Dissipation is associated with mass exchanges between the updraft and downdraft. Additional dissipation can enter through the small-scale mixing terms included on the third line. De Roode et al. (2000) independently noticed the relationship between the lateral mass exchange terms and dissipation rate in their study of a scalar variance equation.

We now perform a similar analysis for the flux equation. This time we expect to find gradient production, in addition to dissipation, transport, and the sourcesink terms. The starting point is (36). The details of the derivation are given by Lappen (1999). The result is

$$\begin{aligned}
& \frac{\partial}{\partial t} m\sigma(1 - \sigma)(w_{\text{up}} - w_{\text{dn}})(h_{\text{up}} - h_{\text{dn}}) \\
&= -(E + D)(w_{\text{up}} - w_{\text{dn}})(h_{\text{up}} - h_{\text{dn}}) \\
&\quad - \frac{\partial}{\partial z} (1 - 2\sigma)(w_{\text{up}} - w_{\text{dn}})M_c(h_{\text{up}} - h_{\text{dn}}) \\
&\quad - M_c(w_{\text{up}} - w_{\text{dn}})\frac{\partial \bar{h}}{\partial z} \\
&\quad + m\sigma(1 - \sigma)(h_{\text{up}} - h_{\text{dn}})[(S_w)_{\text{up}} - (S_w)_{\text{dn}}] \\
&\quad + M_c[(S_h)_{\text{up}} - (S_h)_{\text{dn}}]. \quad (49)
\end{aligned}$$

Here we see both the transport term and the gradient production term. The last term represents the effects of sources and sinks of h (such as the SPS mixing, discussed later) on the flux. The second-to-last term, which involves sources and sinks of the vertical velocity, contributes the important buoyancy term of the flux equation. It also represents the pressure term and the effects on the flux of the subplume mixing of the vertical velocity. The latter are probably negligible.

Finally, to complete the discussion of second moments, we show the plume equation for the variance, h'^2 :

$$\begin{aligned}
& \frac{\partial}{\partial t} m\sigma(1 - \sigma)(h_{\text{up}} - h_{\text{dn}})^2 \\
&= -(E + D)(h_{\text{up}} - h_{\text{dn}})^2 \\
&\quad - \frac{\partial}{\partial z} [M_c(1 - 2\sigma)(h_{\text{up}} - h_{\text{dn}})^2] \\
&\quad - 2M_c(h_{\text{up}} - h_{\text{dn}})\frac{\partial \bar{h}}{\partial z} + 2M_c[(S_h)_{\text{up}} - (S_h)_{\text{dn}}]. \quad (50)
\end{aligned}$$

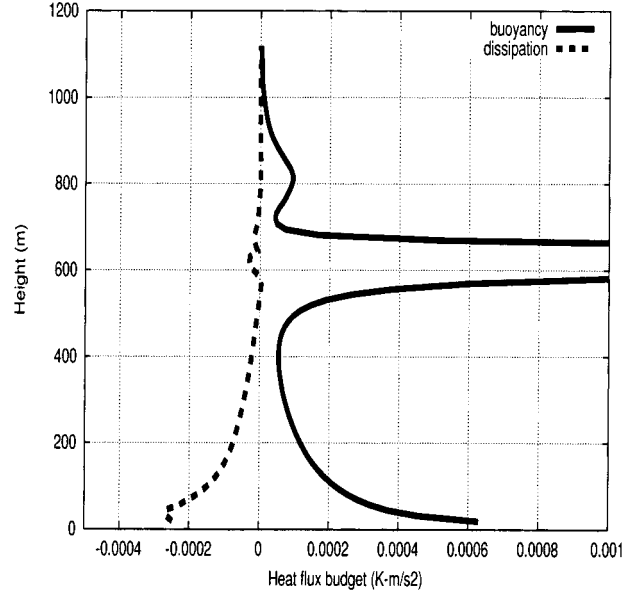


FIG. 2. Comparison of the buoyancy and dissipation terms in the heat flux budget of a convective boundary layer. The plot is from an LES run done by S. de Roode (2000, personal communication).

We hasten to point out that this equation is not explicitly used in ADHOC. In ADHOC, we diagnose h'^2 using the RSM formula given by Eq. (7). Thus, (50) will be implicitly satisfied, provided that the source terms of (48) and (49) are consistently formulated.

Before we move on to the third-moment equations, we elaborate on another key point. The E and D terms in the second-moment equations represent dissipation through mixing of the updraft and downdraft properties. In HOC equations, the dissipation rate for a flux,

$$\frac{\partial \overline{w'h'}}{\partial t} \sim -v \frac{\partial}{\partial z} w' \frac{\partial}{\partial z} h', \quad (51)$$

is typically neglected on the basis that sometimes the product of these spatial derivatives is positive and sometimes it is negative so that the average of the product can be close to zero. While neglect of these terms may be justified for the very small scales (where true molecular dissipation occurs), the fact is that HOC purports to represent, with a single set of statistics, *all* of the scales of the turbulent motion field, including most importantly the large-eddy scales, which are responsible for most of the fluxes. There can be little doubt that the fluxes on large-eddy scales are significantly “dissipated” by the interactions of the large eddies with smaller-scale eddies. Recent LES results (S. de Roode 2000, personal communication) show that this dissipation term is of the same order as the buoyancy term in the lower part of a convective boundary layer. His results are depicted in Fig. 2.

In HOC models, the pressure terms of the flux equations are typically modeled with a return-to-isotropy parameterization (Rotta 1951a,b), which takes the form

of dissipation-like terms involving a proportionality constant. There is uncertainty in the literature over the value of the constant in front of this dissipation-like return-to-isotropy term (Bougeault 1981b). We contend that in HOC models this term actually represents the *combined* effects of flux dissipation and the true pressure term. In ADHOC, we include the effects of both of these terms (see LR2 and section 4).

Finally, we present the equation for the third moment of the vertical velocity as given by Eq. (37). The details of this derivation are given by Lappen (1999). The final result is

$$\begin{aligned}
& \frac{\partial}{\partial t} [m\sigma(1-\sigma)(1-2\sigma)(w_{\text{up}} - w_{\text{dn}})^3] \\
&= (w_{\text{up}} - w_{\text{dn}})^3 [E(3\sigma - 2) + D(3\sigma - 1)] \\
&\quad - (w_{\text{up}} - w_{\text{dn}})^3 [6\sigma^2 - 6\sigma + 1] \\
&\quad \times \frac{\partial}{\partial z} [m\sigma(1-\sigma)(w_{\text{up}} - w_{\text{dn}})] \\
&\quad - \frac{3}{2} m\sigma(1-\sigma)(1-2\sigma)(w_{\text{up}} - w_{\text{dn}})^2 \\
&\quad \times \frac{\partial}{\partial z} [(1-2\sigma)(w_{\text{up}} - w_{\text{dn}})^2] \\
&\quad + 3(1-2\sigma)M_c(w_{\text{up}} - w_{\text{dn}})[(S_w)_{\text{up}} - (S_w)_{\text{dn}}]. \quad (52)
\end{aligned}$$

Here the entrainment and detrainment terms are multiplied by linear functions of σ . We show in LR2 that the E and D terms in (52), despite their different form, still act as dissipation in the $\overline{w'w'w'}$ equation.

In order for the standard HOC and the plume-model equations for $\overline{w'w'w'}$ to be consistent, the third and fourth terms on the right-hand side of (52) must be equal to the first and second terms on the right-hand side of (34), the transport and gradient-production terms, respectively. We can show this by replacing h with w in (7) and (9), plugging the result into the aforementioned terms in (34), and expanding the derivatives [see Lappen (1999) for a derivation].

We can summarize the insight that we have gained from this analysis. First, there is a term-by-term correspondence between the ADHOC plume equations and those of HOC. In this correspondence we see that entrainment and detrainment in ADHOC act as dissipation in the second-moment equations, but they act somewhat differently in the equation for the third moment of the vertical velocity. In these higher-moment plume equations, there are terms that represent “generic” sources and sinks. These sources and sinks include the effects of pressure, buoyancy, and SPS fluxes. We will show in LR2 that the SPS effects are quite important, especially when clouds are present. In LR2, we will also explain in detail how ADHOC parameterizes both the lateral mass exchanges and the SPS fluxes. In the next section, we will examine the ADHOC equations derived

here (using an analysis similar to that of RSM), and show how they specifically encompass both HOC and MFC within a single framework.

c. Limiting cases

We now examine two limiting cases, $\sigma = 1/2$ and $\sigma \ll 1$, which were also discussed by RSM and de Roode et al. (2000). We expect that for $\sigma = 1/2$ local transport dominates. The case $\sigma \ll 1$ is relevant to cumulus convection (e.g., Arakawa and Schubert 1974). Consider the variance equation [Eq. (50)] written in the “mass-flux framework”:

$$\begin{aligned}
\frac{\partial \overline{h'^2}}{\partial t} &= -2 \frac{M_c(h_{\text{up}} - h_{\text{dn}})}{m} \frac{\partial \overline{h}}{\partial z} \\
&\quad - \frac{1}{m} \frac{\partial}{\partial z} [M_c(1-2\sigma)(h_{\text{up}} - h_{\text{dn}})^2] \\
&\quad - (E + D)(h_{\text{up}} - h_{\text{dn}})^2. \quad (53)
\end{aligned}$$

Assuming a quasi-steady state and using (3), we can rewrite (53) as

$$\begin{aligned}
0 &= -2\overline{w'h'} \frac{\partial \overline{h}}{\partial z} - \frac{1}{m} \frac{\partial}{\partial z} [M_c(1-2\sigma)(h_{\text{up}} - h_{\text{dn}})^2] \\
&\quad - \left(\frac{E + D}{m} \right) \left(\frac{\overline{mw'h'}}{M_c} \right)^2. \quad (54)
\end{aligned}$$

Setting $\sigma = 1/2$ in (54), the middle term drops out and we can solve for the flux $\overline{mw'h'}$:

$$\overline{mw'h'} = \frac{-2M_c^2}{E + D} \frac{\partial \overline{h}}{\partial z}. \quad (55)$$

This describes downgradient diffusion, in which the effective eddy diffusivity is represented by

$$K_{\text{eff}} = \frac{2M_c^2}{E + D}. \quad (56)$$

From this exercise, we see that when σ approaches 1/2, the nonlocal transport term (third moment) drops out and the remaining terms describe local diffusion. In this manner, the mass-flux model is able to represent situations in which nonlocal effects play no role.

It is interesting to note that, more than three decades ago, Deardorff (1966) came to this same conclusion. He performed a similar analysis with the HOC variance equation for the potential temperature θ . He determined that, when the triple-correlation transport term is small, and for steady-state conditions, one can solve for the heat flux in terms of the remaining molecular dissipation and radiation terms. The heat flux is directed down the gradient.

A second limiting case is that of cumulus convection ($\sigma \ll 1$). To examine this situation, we rewrite (54) using (3), and the equilibrium assumption

$$-2\overline{w'h'}\frac{\partial\bar{h}}{\partial z} - \frac{1}{m}\frac{\partial}{\partial z}\left[\frac{(\overline{mw'h'})^2}{M_c}(1-2\sigma)\right] - \left(\frac{E+D}{m}\right)\left(\frac{\overline{mw'h'}}{M_c}\right)^2 = 0. \quad (57)$$

In the limit $\sigma \ll 1$, $1 - 2\sigma \approx 1$. Using this in (57), and expanding out the middle term, we get

$$-2\overline{w'h'}\frac{\partial\bar{h}}{\partial z} - \left(\frac{2\overline{w'h'}}{M_c}\right)\frac{\partial}{\partial z}\overline{mw'h'} + \left(\frac{\overline{w'h'}}{M_c}\right)^2\frac{\partial M_c}{\partial z} - \left(\frac{E+D}{m}\right)\left(\frac{\overline{mw'h'}}{M_c}\right)^2 = 0. \quad (58)$$

Equation (58) can be simplified further using the steady-state version of (47),

$$\frac{\partial M_c}{\partial z} = E - D. \quad (59)$$

Using (59) in (58), we get

$$-2\overline{w'h'}\frac{\partial\bar{h}}{\partial z} - 2\left(\frac{\overline{w'h'}}{M_c}\right)\frac{\partial}{\partial z}\overline{mw'h'} - \frac{2D}{m}\left(\frac{\overline{mw'h'}}{M_c}\right)^2 = 0. \quad (60)$$

Multiplying (60) by $-M_c/2\overline{w'h'}$ and solving for $\partial/\partial z\overline{w'h'}$, we get

$$-\frac{\partial}{\partial z}\overline{mw'h'} = M_c\frac{\partial\bar{h}}{\partial z} + D(h_{\text{up}} - h_{\text{an}}). \quad (61)$$

Equation (61) is quite well known in the field of cumulus parameterization. The first term represents the effect of ‘‘compensating subsidence.’’ It acts to warm and dry the environmental air. The second term describes the effect of detrainment on the environment. It is especially important near cloud top. This same equation was derived by AS74, using a very different method.

Wyngaard and Weil (1991) also obtained a result similar to (54). Their Eq. (36) can be written as

$$\frac{\partial\bar{C}}{\partial z} = -\frac{\overline{c'w'}}{K} - \left(\frac{S\sigma_w T_L}{2K}\right)\frac{\partial}{\partial z}\overline{c'w'}, \quad (62)$$

where C is a passive, conservative scalar; K is an eddy diffusivity; S is the skewness of the vertical velocity; $\sigma_w = (\overline{w'^2})^{1/2}$; and T_L is the Lagrangian integral time-scale. This equation contains three terms that are proportional to (in order from left to right) the gradient of the mean scalar, the scalar flux itself, and the scalar-flux divergence. If the last term is negligible, we obtain the downgradient diffusion formula,

$$\overline{c'w'} = -K\frac{\partial\bar{C}}{\partial z}. \quad (63)$$

This is analogous to our Eq. (55) derived for the case

where $\sigma = 1/2$. If the middle term in (62) is negligible, we get

$$\frac{\partial}{\partial z}\overline{c'w'} = -\left(\frac{2K}{S\sigma_w T_L}\right)\frac{\partial\bar{C}}{\partial z}. \quad (64)$$

This is similar to our Eq. (61), but without the detrainment term, for the case where $\sigma \ll 1$.

3. Momentum fluxes

MFC can succeed when there is a strong correlation between the vertical velocity and the variable of interest, as is typically the case for thermodynamic variables in convective layers. However, high correlations are not always found between the vertical velocity and the dynamic quantities (zonal and meridional momentum). In a free-convective boundary layer, mass continuity dictates that u' and v' are largest *in between* the updraft and downdrafts (where w' is near zero) and are smallest in the centers of the updrafts and downdrafts (where w' is a maximum) (Fig. 3a). This does not bode well for an accurate determination of the momentum fluxes with MFC. In a shear-driven boundary layer, however, the correlation between u' and w' is strong (Fig. 3b), and we may very well be able to use the mass-flux method with accurate results. The only PBL study (that we are aware of) that tested the representation of momentum fluxes with a mass-flux decomposition was that of Khalsa and Greenhut (1985). They showed that this formulation is valid for momentum fluxes in the lower third of the marine boundary layer. However, this study is quite limited in its range of applicability and, to our knowledge, has not been extended to other regimes.

One could argue that, given the fact that momentum fluxes are weak (and relatively unimportant) in the convective boundary layer, the ‘‘noncorrelation’’ is harmless. This, combined with the fact that u' and w' are well correlated in the shear-driven boundary layer, may indicate that ADHOC could still produce accurate momentum fluxes, *when and where the fluxes are large*. While this may be true, we have chosen to prognose the momentum fluxes (as we do the thermodynamic fluxes) but use ‘‘downgradient’’ diffusion for the third-moment transport terms in these equations. ADHOC predicts $u'x'$, $w'u'$, $u'u'$ (as well as the analogous v' moments; here x represents any thermodynamic variable) using conventional HOC methods; the details are described by Lappen (1999).

4. Pressure terms

Pressure effects enter the ADHOC equations through the vertical velocity ‘‘source’’ terms [e.g., $(S_w)_{\text{up}} - (S_w)_{\text{dn}}$ in Eq. (39)]. Up to now, the pressure terms have been dealt with very differently in MFC and HOC. The pressure-term parameterizations have always been an integral part of HOC models. On the other hand, few

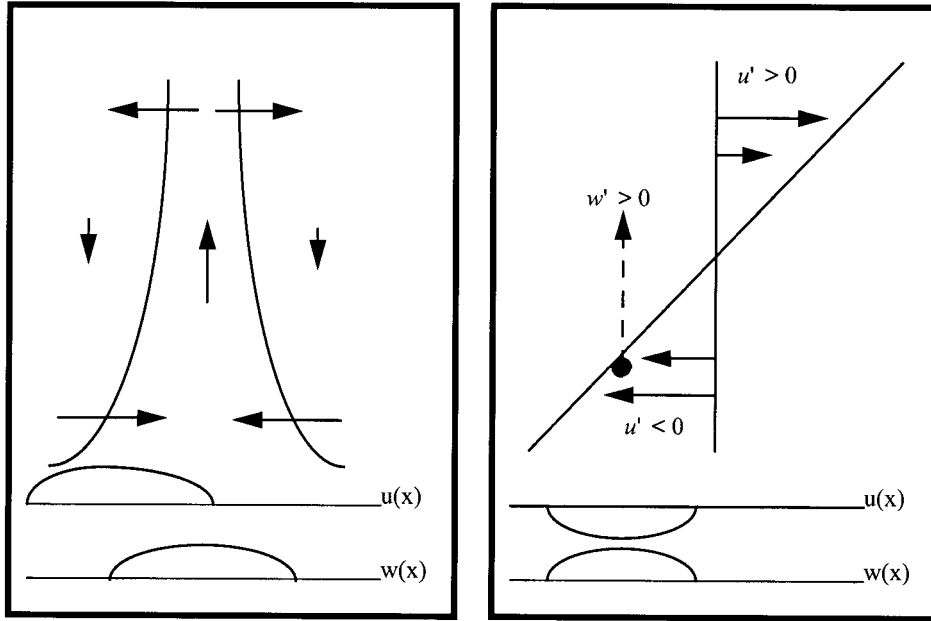


FIG. 3. The correlation of w and u in (left) the convective boundary layer and (right) the shear-driven boundary layer. We see that w and u are correlated in (right) but are 90° out of phase in (left).

mass-flux models have even considered these terms [an exception is the study of Wu and Yanai (1994)]. It may be possible to use the anelastic pressure equation (Holton 1973; Yau 1979; Lappen 1999) to derive the updraft and downdraft pressure gradient components, and substitute this directly into Eq. (40). However, the current version of ADHOC makes use of ideas from the HOC literature. Following Rotta (1951) and Launder (1975), we write

$$p' \left(\frac{\partial u'_i}{\partial x_k} + \frac{\partial u'_k}{\partial x_i} \right) = -C_1 \frac{q}{l} \left(\overline{u'_i u'_k} - \delta_{ij} \frac{q^2}{3} \right) - C_2 \left(P_{ij} - \frac{2}{3} \delta_{ij} P \right), \quad (65)$$

where

$$P_{ij} \equiv - \left(\overline{u'_i u'_k} \frac{\partial \overline{U}_j}{\partial x_k} + \overline{u'_j u'_k} \frac{\partial \overline{U}_i}{\partial x_k} \right) - \frac{\alpha}{T} \left(\overline{u'_i T' g_j} + \overline{u'_j T' g_i} \right), \quad \text{and} \quad (66)$$

$$P \equiv - \left(\overline{u'_i u'_k} \frac{\partial \overline{U}_i}{\partial x_k} + \frac{\alpha}{T} \overline{u'_i T' g_i} \right). \quad (67)$$

Here α is the coefficient of thermal expansion, T is the temperature, θ is the potential temperature, and l is a turbulent length scale (Blackadar 1962).

Using (40) and (3), we can write out the ADHOC formula for the pressure term in the $w'w'$ equation [Eq. (48)],

$$\begin{aligned} & \frac{\partial}{\partial t} [m\sigma(1 - \sigma)(w_{\text{up}} - w_{\text{dn}})^2] \\ & \sim -2\sigma(1 - \sigma)(w_{\text{up}} - w_{\text{dn}}) \frac{\partial}{\partial z} (p_{\text{up}} - p_{\text{dn}}). \end{aligned} \quad (68)$$

We can rewrite this as

$$\begin{aligned} & \frac{\partial}{\partial t} [m\sigma(1 - \sigma)(w_{\text{up}} - w_{\text{dn}})^2] \\ & \sim -2 \frac{\partial}{\partial z} \left[\frac{M_c}{m} (p_{\text{up}} - p_{\text{dn}}) \right] + 2(p_{\text{up}} - p_{\text{dn}}) \frac{\partial}{\partial z} \left(\frac{M_c}{m} \right). \end{aligned} \quad (69)$$

In the current version of ADHOC, we essentially neglect the first term on the right-hand side of (69) (the pressure transport) and parameterize the second term using the right-hand side of (65).

In summary, for the $u'u'$, $v'v'$, and $w'w'$ equations, we use (65) with l calculated using a modified version of the method of Bougeault and André (1986; see LR2), and with $C_1 = 2.0$, and $C_2 = 0.6$. In the flux equations, we neglect all pressure contributions from (65) except for the first term, which represents the “slow,” return-to-isotropy part:

$$\frac{\partial}{\partial t} \overline{w'w'x'} = -C \frac{q}{l} \overline{w'w'x'}, \quad (70)$$

where x is any variable, $C = 4.85$ for thermodynamic fluxes, and $C = 4.5$ for momentum fluxes. In the $w'w'w'$ equation, we use a form analogous to (70) with $C = 6.5$ (Bougeault 1981b). The limitations of parameterizing pressure effects in this manner are discussed

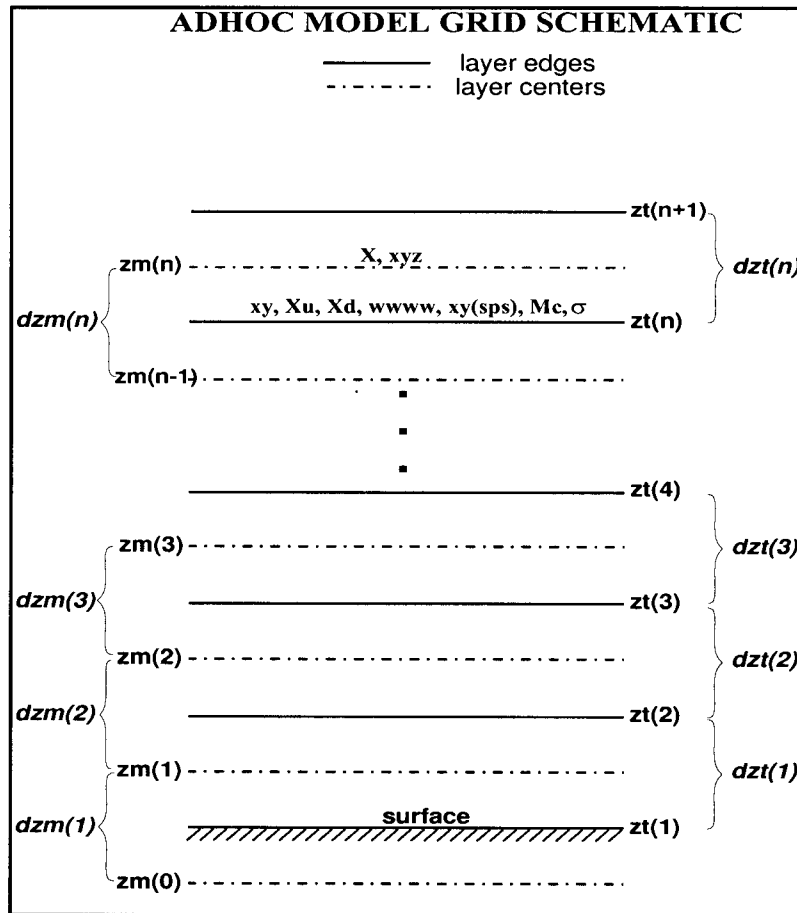


FIG. 4. Vertically staggered grid of the model. The mean state and third moments are defined at the layer centers (zm) while the second and fourth moments are defined at the layer edges (zt). In addition, all mass-flux and subplume-scale (SPS) quantities are defined at the layer edges. Above, small letters represent turbulent quantities and capitals represent the mean state values. Here x, y, and z are dummy symbols representing any model thermodynamic or dynamic variable, and Xu (Xd) represents an updraft (downdraft) quantity.

in LR3. For a further discussion of the pressure terms see Lappen (1999).

5. Boundary conditions

Depending on the application (see LR3), the surface fluxes are either prescribed from observations or else diagnosed following Louis (1979); they are fed directly into the plume-scale motion. Following Krueger (1985), we define all second moments at layer edges and first and third moments at layer centers (see Fig. 4). With the exception of the surface fluxes, we set all second and third moments to zero at the surface. For the first layer above the surface, we predict all first- and second-moment quantities. We prescribe $\overline{w'w's'_v}$ in the middle of the first layer according to the surface layer similarity relationship of Moeng and Wyngaard (1989):

$$\overline{w'w's'_v} = 0.3w^*w^*s_v^* \quad \text{if } \overline{w's'_{v-sfc}} > 0 \quad \text{and} \quad (71)$$

$$\overline{w'w's'_v} = 0 \quad \text{if } \overline{w's'_{v-sfc}} < 0, \quad (72)$$

where w^* is the convective velocity scale and $s_v^* = (\overline{w's'_{v-sfc}}/w^*)$. We diagnose all other third moments using a mass-flux formula analogous to Eq. (8). Because all of the quantities on the right-hand side of Eq. (8) are defined at the layer edges and the third moment is defined at the layer center (Fig. 4), we do an arithmetic average of σ , $(h_{up} - h_{dn})$, and $(w_{up} - w_{dn})$ between the surface and the top of the first layer. In doing so, we use $(w_{up} - w_{dn}) = (h_{up} - h_{dn}) = 0$ and $\sigma = 1/2$ at the surface.

Upper boundary conditions are described by Lappen (1999).

6. Summary and conclusions

In this paper, we have taken the familiar plume equations describing the mean properties of updrafts and downdrafts and used the framework of RSM to derive a set of higher-order prognostic equations. We obtain a hybrid MFC-HOC model (called ADHOC) whose equa-

TABLE 1. Comparison of ADHOC with the mass-flux models of Wang and Albrecht (1986) and Arakawa and Schubert (1974).

	ADHOC	Wang and Albrecht (1986)	Arakawa and Schubert (1974)
Vertical velocity equation	The equation for $w_{\text{up}} - w_{\text{dn}}$ is explicitly used in all higher-moment prognostic equations.	Not included	Not included
Parameterization of E and D	E and D are shown to be related to dissipation and are parameterized using a modified form of Bougeault (1986).	Not discussed	The fractional entrainment rate (λ) is considered to be constant for a given cloud type, while detrainment is assumed to occur only at cloud top in order to satisfy mass continuity.
	E and D are positive everywhere in the cloud.	N/A	D is zero everywhere except at cloud top.
	Only one updraft and downdraft are considered.	N/A	Many categories of updrafts and downdrafts are considered.
σ equation	The prognostic σ equation is given by Eq. (47).	Not discussed	The σ equation is used with the assumption that σ is in steady state.
Subplume-scale effects	Subplume-scale effects are considered in the mean-state and second-moment equations using a modified version of Deardorff (1980) to predict the subplume-scale turbulent kinetic energy.	Not discussed	Not discussed
Pressure parameterization	ADHOC uses the HOC pressure parameterization given by Rotta (1951a,b) and Launder (1975).	Not discussed	Not discussed
Type of regimes considered	Boundary layer and shallow convection	Boundary layer and S \acute{c} convection	Shallow and deep convection, excluding the boundary layer.

tions are term-by-term consistent with the corresponding conventional HOC equations. A comparison of the features of ADHOC with those of two other mass-flux models is given in Table 1. GCMs use a “modular” approach toward parameterizing cloud and the boundary layer processes; as a result, they have trouble with transitional regimes. ADHOC may be a step toward unifying parameterizations of cloud and boundary layer processes in large-scale models.

ADHOC provides a method to diagnose σ and M_c when $\overline{w'w'}$ and $\overline{w'w'w'}$ are known. The ADHOC equations are derived by integrating the prognostic HOC equations over a top hat PDF, thus guaranteeing consistency with the mass-flux model. In addition, since all higher-moment statistics are derived from the same PDF, there are no realizability issues with this model.

The basic logic behind the ADHOC approach is sketched in Figs. 1 and 5, and can be summarized as follows.

- 1) Prognose (or initialize) $\overline{w'w'}$ and $\overline{w'w'w'}$ using the unified MFC–HOC equations [Eqs. (48) and (52)].
- 2) Use these prognosed values to diagnose σ , M_c [Eqs. (10) and (11)], and the properties of the updraft and downdraft.
- 3) Predict (or initialize) the fluxes.
- 4) Use the thermodynamic fluxes, along with M_c , to diagnose the properties of the updraft and downdrafts [Eq. (3)].
- 5) Diagnose higher-order moments using the RSM formulation [Eqs. (7)–(9)].

- 6) Calculate the SPS fluxes and the radiative forcing (done separately for the updraft and downdrafts).
- 7) Update the surface fluxes, diagnose the lateral mixing terms (E and D).

We have chosen to predict $\overline{w'w'}$, $\overline{w'w'w'}$, the fluxes, and the mean-state quantities. We could reasonably choose various other combinations of prognostic equations to form a model that would be mathematically equivalent to that described above. For example, we could use the same set of prognostic equations described above with the exception that we predict σ [using Eq. (47)] and diagnose $\overline{w'w'w'}$. Similarly, we could choose not to predict the fluxes, but instead use prognostic equations for the “updraft minus downdraft” quantities [i.e., equations of the form of (38)]; in such a model, we would compute the fluxes using Eq. (3).

One weakness of the current model is that the tophat PDF cannot fully describe the statistics of the flow; it is an oversimplification. To make the approach more accurate, a more realistic PDF must be used. The ADHOC approach can be generalized to make use of a more realistic PDF.

- 1) Assume a PDF shape, formulated in terms of a few parameters.
- 2) Integrate the prognostic equations over the PDF to get a “plume” model.
- 3) Make mechanistic assumptions in the framework of the plume model (e.g., make assumptions about the lateral mixing).

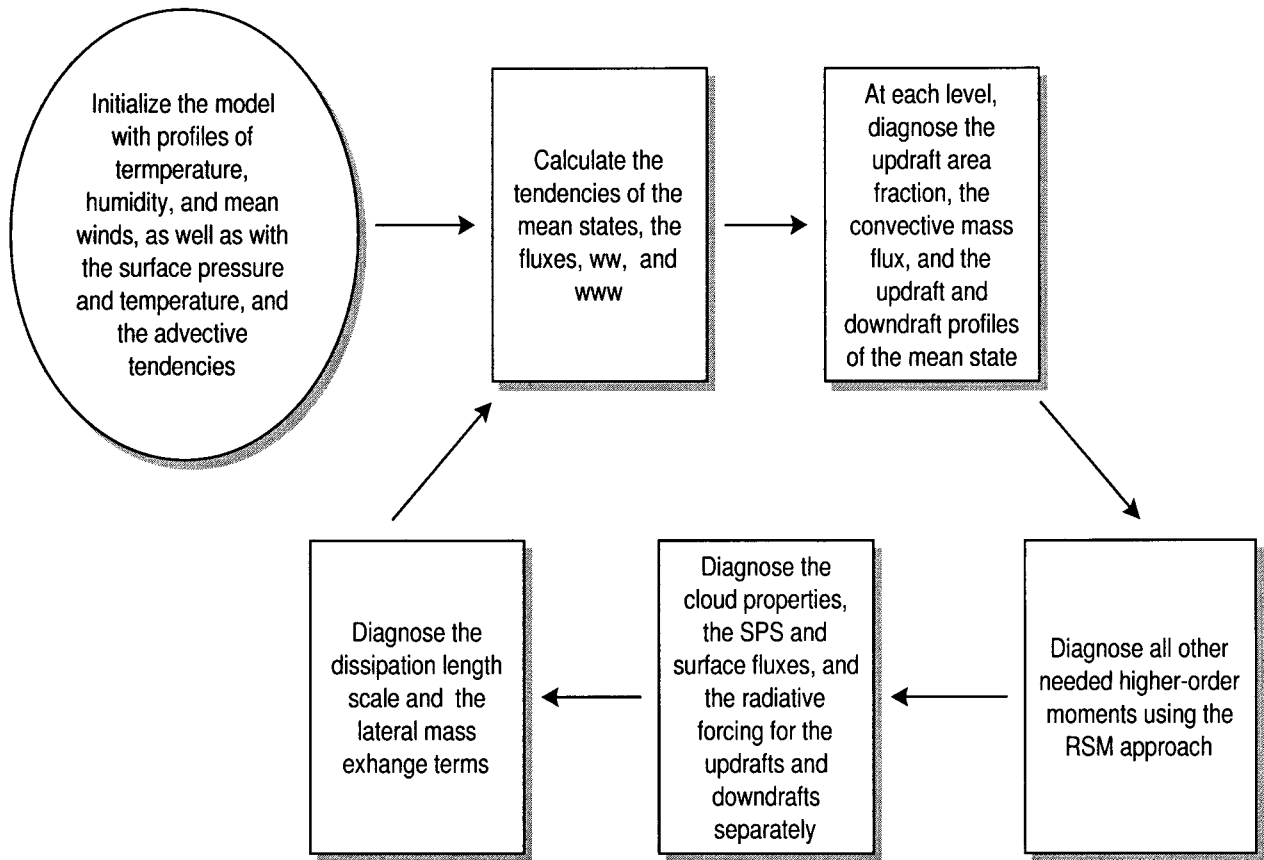


FIG. 5. Model flowchart.

- 4) Derive higher-moment equations from the plume model.
- 5) Diagnose the parameters that describe the PDF shape from the predicted moments.

We can actually go from step 1 to step 4 directly for some of the terms. For example, in the current version of ADHOC, the thermodynamic variances can be diagnosed directly from the PDF once the PDF is known.

One result that emerges from our analysis is that the lateral mass exchange terms (E and D) are analogous to the dissipation terms in the corresponding “standard” HOC equations. In LR2, we discuss parameterizations of E and D . Also in LR2, we discuss the parameterization of SPS fluxes, which contribute to the source/sink terms such as S_w [see Eq. (40)]. The SPS fluxes allow us to account for the portion of the turbulent motion that is *not* represented with the tophat PDF.

A weakness of the current model is its treatment of momentum. The mass-flux model lacks any information on the tilt of the convection, which controls momentum fluxes through the covariance of u' (and v') with w' . We have chosen to use conventional HOC to prognose the momentum fluxes. Ideally, a formulation consistent with the assumed statistical PDF (tophat in the current

model) should be used for higher-moment momentum terms.

The pressure terms of the model are currently based on conventional HOC ideas. We are exploring an alternative approach based on the plume model.

With ADHOC, the additional complexity introduced by prognosing the higher moments is offset by the prospect of simplifying the model by unifying its convection and boundary layer parameterizations. The number of equations used by ADHOC is significantly less than would be required with a full second-order closure model.

Despite the step that we have taken here to unify cloud and boundary layer processes, a few aspects of the current model must be changed before incorporation into a large-scale model is realistic. First of all, the current model uses σ to define the fractional area of the updrafts. However, σ can only determine the ratio of the updraft-to-downdraft areas, not the actual number of or spacing between updrafts. Even when the convection is of a single type, at least two horizontal length scales should be considered: one for the size of the individual updrafts and one for the mean distance between updrafts.

The second aspect of the current model that must be

addressed before its incorporation into a large-scale model is resolution. ADHOC's need for high vertical and temporal resolution is one of the main factors inhibiting its incorporation into a GCM. In particular, high resolution is needed near the PBL top where properties of the PBL change rapidly across the PBL-top inversion. One way to alleviate this problem is to use a modified σ coordinate (Suarez et al. 1983) in which high resolution near the PBL top is not needed because the PBL top is a coordinate surface.

We believe that ADHOC has the potential to provide a unified parameterization of cumulus and boundary layer processes. Our hope is that by generalizing the PDF we can derive a more realistic, more flexible model. Our long-term goal is a unified parameterization that will combine the PBL and cumulus parameterizations in a single physical and computational framework.

Acknowledgments. This research was funded by the National Aeronautics and Space Administration under Grant NAGI-1701 and Contract 960700 through the Jet Propulsion Laboratory, and by the National Science Foundation under Grant OPP9504246, all to Colorado State University. Computing support was obtained from the Scientific Computing Division of the National Center for Atmospheric Research. Prof. S. Krueger of the University of Utah made helpful suggestions along the way. Stephan de Roode from the University of Washington provided the LES results shown in Fig. 2. We would also like to thank Akio Arakawa and two anonymous reviewers for their helpful suggestions.

REFERENCES

- Albrecht, B. A., 1979: A model of the thermodynamic structure of the trade-wind boundary-layer. Part II. Applications. *J. Atmos. Sci.*, **36**, 90–98.
- André, J. C., G. DeMoor, P. Lacarrere, and R. DuVachat, 1976: Turbulence approximation for inhomogeneous flows: Part I. The clipping approximation. *J. Atmos. Sci.*, **33**, 476–481.
- , —, G. Therry, and R. Du Vachat, 1978: Modeling the 24-hour evolution of the mean and turbulent structures of the planetary boundary layer. *J. Atmos. Sci.*, **35**, 1861–1883.
- Arakawa, A., 1969: Parameterization of cumulus convection. *Proc. WMO/IUGG Symp. Numerical Weather Prediction*, Tokyo, Japan, Japan Meteorological Agency, 1–6.
- , and W. H. Schubert, 1974: The interaction of a cumulus cloud ensemble with the large-scale environment, Part I. *J. Atmos. Sci.*, **31**, 674–701.
- Ball, F. K., 1960: Control of inversion height by surface heating. *Quart. J. Roy. Meteor. Soc.*, **86**, 483–494.
- Bechtold, P., J. W. M. Cuijpers, P. Mascart, and P. Trouilhet, 1995: Modeling of trade wind cumuli with a low-order turbulence model: Toward a unified description of Cu and Sc clouds in meteorological models. *J. Atmos. Sci.*, **52**, 455–463.
- Beljaars, A. C. M., J. L. Walmsley, and P. A. Taylor, 1987: Modeling of turbulence over low hills and varying surface roughness. *Bound.-Layer Meteor.*, **41**, 203–215.
- Benoit, R., 1976: A comprehensive parameterization of the atmospheric boundary-layer for general circulation models. Ph.D. dissertation, McGill University, and National Center for Atmospheric Research cooperative thesis No. 39, 278 pp.
- Berkowicz, R., and P. L. Prahm, 1979: Generalization of K theory for turbulent diffusion. Part I: Spectral turbulent diffusivity concept. *J. Appl. Meteor.*, **18**, 266–272.
- Betts, A., 1973: Non-precipitating cumulus convection and its parameterization. *Quart. J. Roy. Meteor. Soc.*, **99**, 178–196.
- , 1976: Modeling subcloud layer structure and interaction with a shallow cumulus layer. *J. Atmos. Sci.*, **33**, 2363–2382.
- Blackadar, A. K., 1962: The vertical distribution of wind and turbulent exchange in neutral atmospheres. *J. Geophys. Res.*, **67**, 3095–3102.
- Bougeault, P., 1981a: Modeling the trade wind cumulus boundary layer. Part. I: Testing the ensemble cloud relations against numerical data. *J. Atmos. Sci.*, **38**, 2414–2428.
- , 1981b: Modeling the trade wind cumulus boundary layer. Part. II: A high-order one-dimensional model. *J. Atmos. Sci.*, **38**, 2429–2439.
- , and J. C. André, 1986: On the stability of the third-order turbulence closure for the modeling of the stratocumulus-topped boundary layer. *J. Atmos. Sci.*, **43**, 1574–1581.
- Businger, J. A., and S. P. Oncley, 1990: Flux measurements with conditional sampling. *J. Atmos. Oceanic Technol.*, **7**, 349–352.
- Canuto, V. M., 1992: Turbulent convection with overshooting: Reynolds stress approach. *Astrophys. J.*, **392**, 218–232.
- , F. Minotti, C. Ronchi, R. M. Ypma, and O. Zeman, 1994: Second-order closure PBL model with new third-order moments: Comparison with LES data. *J. Atmos. Sci.*, **51**, 1605–1618.
- Chatfield, R. B., and R. A. Brost, 1987: Two-stream model of the vertical transport of trace species in the convective boundary layer. *J. Geophys. Res.*, **92** (D11), 13 263–13 276.
- Crum, T. D., R. B. Stull, and E. W. Eloranta, 1987: Coincident lidar and aircraft observations of entrainment into thermals and mixed layers. *J. Climate Appl. Meteor.*, **26**, 774–788.
- Deardorff, J. W., 1966: The counter-gradient heat flux in the lower atmosphere and in the laboratory. *J. Atmos. Sci.*, **23**, 503–506.
- , 1980: Stratocumulus-capped mixed layers derived from a three-dimensional model. *Bound.-Layer Meteor.*, **18**, 495–527.
- de Laat, A. T. J., and P. G. Duynkerke, 1998: Analysis of ASTEX-stratocumulus observational data using mass-flux approach. *Bound.-Layer Meteor.*, **86**, 63–87.
- de Roode, S. R., P. G. Duynkerke, and A. P. Siebesma, 2000: Analogies between mass-flux and Reynolds-averaged equations. *J. Atmos. Sci.*, **57**, 1585–1598.
- Detering, H. W., and D. Etling, 1985: Application of the $E-\epsilon$ turbulence model to the atmospheric boundary layer. *Bound.-Layer Meteor.*, **33**, 113–133.
- Greenhut, G. K., and S. Khalsa, 1982: Updraft and downdraft events in the atmospheric boundary layer over the equatorial Pacific Ocean. *J. Atmos. Sci.*, **39**, 1803–1818.
- , and —, 1987: Convective elements in the marine atmospheric boundary layer. Part 1: Conditional sampling statistics. *J. Climate Appl. Meteor.*, **26**, 813–822.
- Hanson, H. P., 1981: On mixing by tradewind cumuli. *J. Atmos. Sci.*, **38**, 1003–1014.
- Holton, J. R., 1973: A one-dimensional cumulus model including pressure perturbations. *Mon. Wea. Rev.*, **101**, 201–205.
- Holtzlag, A. A. M., and C.-H. Moeng, 1991: Eddy diffusivity and countergradient transport in the convective atmospheric boundary layer. *J. Atmos. Sci.*, **48**, 1690–1698.
- , and B. A. Boville, 1993: Local versus nonlocal boundary-layer diffusion in a global climate model. *J. Climate*, **6**, 1825–1842.
- Keller, L. V., and A. A. Friedman, 1924: Differentialgleichung für die turbulente Bewegung einer kompressiblen Flüssigkeit. *Proc. First Int. Congr. Appl. Mech.*, Delft, Netherlands, 395–405.
- Khalsa, S. J. S., and G. K. Greenhut, 1985: Conditional sampling of updrafts and downdrafts in the marine atmospheric boundary layer. *J. Atmos. Sci.*, **42**, 2550–2562.
- Krueger, S. K., 1985: Numerical simulation of tropical cumulus clouds and their interaction with the subcloud layer. Ph.D. thesis, University of California, Los Angeles, 205 pp.
- Langland, R. H., and C.-S. Liou, 1996: Implementation of an $E-\epsilon$

- parameterization of vertical subgrid-scale mixing in a regional model. *Mon. Wea. Rev.*, **124**, 905–918.
- Lappen, C.-L., 1999: The unification of mass flux and higher-order closure in the simulation of boundary layer turbulence. Ph.D. thesis, Colorado State University, 330 pp.
- , and D. A. Randall, 2001a: Toward a unified parameterization of the boundary layer and moist convection. Part II: Lateral mass exchanges and subplume-scale fluxes. *J. Atmos. Sci.*, **58**, 2037–2051.
- , and —, 2001b: Toward a unified parameterization of the boundary layer and moist convection. Part III: Simulations of clear and cloudy convection. *J. Atmos. Sci.*, **58**, 2052–2072.
- Lauder, B. E., 1975: On the effects of a gravitational field on the turbulent transport of heat and momentum. *J. Fluid Mech.*, **67**, 569–581.
- Lenshow, D. H., and P. L. Stephens, 1980: Role of thermals in the convective boundary layer. *Bound.-Layer Meteor.*, **19**, 509–532.
- Lilly, D. K., 1968: Models of cloud-topped mixed layers under a strong inversion. *Quart. J. Roy. Meteor. Soc.*, **94**, 292–309.
- Louis, J.-F., 1979: Parametric model of vertical eddy fluxes in the atmosphere. *Bound.-Layer Meteor.*, **17**, 187–202.
- Lumley, J. L., 1978: Computational modeling of turbulent flows. *Advances in Applied Mechanics*, Academic Press, 123–176.
- , and B. Khajeh Nouri, 1974: Computational modeling of turbulent transport. *Advances in Geophysics*, Vol. 18A, Academic Press, 169–192.
- Mailhot, J., and R. Benoit, 1982: Finite-element model of the atmospheric boundary layer suitable for use with numerical weather prediction models. *J. Atmos. Sci.*, **39**, 2249–2266.
- Moeng, C.-H., and J. C. Wyngaard, 1989: Evaluation of turbulent transport and dissipation closures in second-order modeling. *J. Atmos. Sci.*, **46**, 2311–2330.
- Naot, D., A. Shavit, and M. Wolfshtein, 1973: Two-point correlation model and the redistribution of Reynolds stresses. *Phys. Fluids*, **16**, 738–743.
- Nicholls, S., and M. A. Lemone, 1980: Fair weather boundary layer in GATE: The relationship of subcloud fluxes and structure to the distribution and enhancement of cumulus clouds. *J. Atmos. Sci.*, **37**, 2051–2067.
- Ooyama, K., 1971: A theory on parameterization of cumulus clouds. *J. Meteor. Soc. Japan*, **49**, 744–856.
- Penc, R. S., and B. Albrecht, 1987: Parametric representation of heat and moisture fluxes in cloud-topped mixed layers. *Bound.-Layer Meteor.*, **38**, 225–248.
- Randall, D. A., 1976: The interaction of the planetary boundary-layer with large-scale circulations. Ph.D. thesis, University of California, Los Angeles, 247 pp.
- , 1987: Turbulent fluxes of liquid water and buoyancy in partly cloudy layers. *J. Atmos. Sci.*, **44**, 850–858.
- , and B. A. Wielicki, 1997: Measurements, models, and hypotheses in the atmospheric sciences. *Bull. Amer. Meteor. Soc.*, **78**, 399–406.
- , Q. Shao, and C.-H. Moeng, 1992: A second-order bulk boundary-layer model. *J. Atmos. Sci.*, **49**, 1903–1923.
- Rotta, J. C., 1951a: Statistische Theorie nichthomogener Turbulenz 1. *Z. Phys.*, **129**, 547–572.
- , 1951b: Statistische Theorie nichthomogener Turbulenz 2. *Z. Phys.*, **131**, 51–77.
- Schumann, U., and C.-H. Moeng, 1991a: Plume fluxes in clear and cloudy convective boundary layers. *J. Atmos. Sci.*, **48**, 1746–1757.
- Siebesma, A. P., and J. W. M. Cuijpers, 1995: Evaluation of parametric assumptions for shallow cumulus convection. *J. Atmos. Sci.*, **52**, 650–666.
- Somméria, G., 1976: Three-dimensional simulation of turbulent processes in an undisturbed trade wind boundary layer. *J. Atmos. Sci.*, **33**, 216–241.
- Stull, R. B., 1988: *An Introduction to Boundary Layer Meteorology*. Kluwer Academic, 666 pp.
- Suarez, M. J., A. Arakawa, and D. A. Randall, 1983: The parameterization of the planetary boundary layer in the UCLA general circulation model: Formulation and results. *Mon. Wea. Rev.*, **111**, 2225–2243.
- Therry, G., and P. Lecarrère, 1983: Improving the eddy kinetic energy model for planetary boundary layer description. *Bound.-Layer Meteor.*, **25**, 63–88.
- Troen, I., and L. Mahrt, 1986: A simple model of the atmospheric boundary layer: Sensitivity to surface evaporation. *Bound.-Layer Meteor.*, **37**, 129–148.
- Wang, S., and B. Albrecht, 1986: Stratocumulus model with an internal circulation. *J. Atmos. Sci.*, **43**, 2374–2391.
- , and —, 1990: A mean gradient of the convective boundary-layer. *J. Atmos. Sci.*, **47**, 126–138.
- , and B. Stevens, 2000: Top-hat representation of turbulence statistics in cloud-topped boundary layers: A large-eddy simulation study. *J. Atmos. Sci.*, **57**, 423–441.
- Wu, X., and M. Yanai, 1994: Effects of vertical wind shear on the cumulus transport of momentum: Observations and parameterizations. *J. Atmos. Sci.*, **51**, 1640–1660.
- Wyngaard, J. C., and O. R. Coté, 1974: The evolution of a convective planetary boundary layer. *Bound.-Layer Meteor.*, **7**, 289–308.
- , and J. C. Weil, 1991: Transport asymmetry in skewed turbulence. *Phys. Fluids*, **3**, 155–161.
- , and C.-H. Moeng, 1992: Parameterizing turbulent diffusion through the joint probability density. *Bound.-Layer Meteor.*, **60**, 1–13.
- Yau, M. K., 1979: Perturbation pressure and cumulus convection. *J. Atmos. Sci.*, **36**, 690–694.
- Young, G. S., 1988a: Turbulence structure of the convective boundary layer. Part I: Variability of normalized turbulence statistics. *J. Atmos. Sci.*, **45**, 719–726.
- , 1988b: Turbulence structure of the convective boundary layer. Part II: Phoenix 78 aircraft observations of thermals and their environment. *J. Atmos. Sci.*, **45**, 727–735.
- Zeman, O., and J. J. Lumley, 1976: Modeling buoyancy driven mixed layers. *J. Atmos. Sci.*, **33**, 1974–1988.